J Ind Microbiol Biotechnol (2015) 42:949–963
DOI 10.1007/s10295-015-1611-z

SYSTEMS BIOTECHNOLOGY

Comparative metabolic profiling reveals the key role of amino acids metabolism in the rapamycin overproduction by *Streptomyces hygroscopicus*

Baohua Wang[1,2] · Jiao Liu[1,2] · Huanhuan Liu[1,2] · Di Huang[3,4] · Jianping Wen[1,2]

Received: 31 January 2015 / Accepted: 23 March 2015 / Published online: 4 April 2015

Abstract Rapamycin is an important natural macrolide antibiotic with antifungal, immunosuppressive and anticancer activity produced by *Streptomyces hygroscopicus*. In this study, a mutant strain obtained by ultraviolet mutagenesis displayed higher rapamycin production capacity compared to the wild-type *S. hygroscopicus* ATCC 29253. To gain insights into the mechanism of rapamycin overproduction, comparative metabolic profiling between the wild-type and mutant strain was performed. A total of 86 metabolites were identified by gas chromatography–mass spectrometry. Pattern recognition methods, including principal component analysis, partial least squares and partial least squares discriminant analysis, were employed to determine the key biomarkers. The results showed that 22 potential biomarkers were closely associated with the increase of rapamycin production and the tremendous metabolic difference was observed between the two strains. Furthermore, metabolic pathway analysis revealed that amino acids metabolism played an important role in the synthesis of rapamycin, especially lysine, valine, tryptophan, isoleucine, glutamate, arginine and ornithine. The inadequate supply of amino acids, or namely "nitrogen starvation" occurred in the mutant strain. Subsequently, the exogenous addition of amino acids into the fermentation medium of the mutant strain confirmed the above conclusion, and rapamycin production of the mutant strain increased to 426.7 mg/L after adding lysine, approximately 5.8-fold of that in the wild-type strain. Finally, the results of real-time PCR and enzyme activity assays demonstrated that dihydrodipicolinate synthase involved with lysine metabolism played vital role in the biosynthesis of rapamycin. These findings will provide a theoretical basis for further improving production of rapamycin.

Keywords Metabolomics · Exogenous feeding strategy · Real-time PCR · Enzyme activity assays · Dihydrodipicolinate synthase

Electronic supplementary material The online version of this article (doi:10.1007/s10295-015-1611-z) contains supplementary material, which is available to authorized users.

B. Wang and J. Liu have contributed equally to this work.

✉ Jianping Wen
jpwen@tju.edu.cn

[1] Key Laboratory of Systems Bioengineering (Ministry of Education), Tianjin University, Tianjin 300072, People's Republic of China

[2] SynBio Research Platform, Collaborative Innovation Center of Chemical Science and Engineering (Tianjin), School of Chemical Engineering and Technology, Tianjin University, Tianjin 300072, People's Republic of China

[3] Key Laboratory of Molecular Microbiology and Technology, Ministry of Education, TEDA Institute of Biological Sciences and Biotechnology, Nankai University, 23 Hongda Street, TEDA, Tianjin 300457, People's Republic of China

[4] Tianjin Key Laboratory of Microbial Functional Genomics, TEDA, Tianjin 300457, People's Republic of China

Introduction

Rapamycin (Sirolimus), produced by *Streptomyces hygroscopicus*, is a 31-membered macrocyclic natural product with various biological and pharmacological activities, such as antifungal, immunosuppressive and antitumor [3, 13, 35]. It should be noted that rapamycin shows lower toxicity and more powerful clinical activity than cyclosporine. With the widespread clinical application and promising prospects, rapamycin has recently attracted much attention of many researchers and pharmaceutical companies.

So far, considerable efforts have been made to improve rapamycin production, such as fermentation technology optimization [7, 26, 27], traditional strains mutation [8, 46, 50], and protoplast-related techniques [5]. Notably, ultraviolet mutagenesis, as a traditional method, has been successfully applied in the field of microbial breeding. However, traditional method is a tedious, laborious and unpredictable process with long period. Nowadays, the low yield of rapamycin still is a bottleneck for further industrialization and commercialization. This problem results from the lack of means for efficiently targeting the key enzymes as well as the poor knowledge on mechanism of rapamycin overproduction. Fortunately, several reports have been published on analysis of the overproduction mechanism in different mutant strains [48]. It is worth noting that metabolic profiling analysis has become a reliable method to investigate the enhancement mechanism of target products in the mutant strain and guide the further rational strategy for strain improvement. For example, Yu et al. [47] used gas chromatography–mass spectrometry (GC–MS)-based metabolomics to reveal metabolic differences between the mutant and wild-type strain of *Rhizopus oryzae*, and the findings provided new insights into the link between high-yielding fumaric acid strain and specific cellular metabolism. Additionally, real-time quantitative PCR coupled with enzyme activity assays was complemented to provide deeper insights into cellular metabolic mechanism. Chen et al. [4] combined real-time PCR and enzyme kinetic analysis approaches, and discovered transaldolase was a rate-limiting enzyme of xylose metabolism in the pentose phosphate pathway for improving bioethanol by *Pichia stipites*. Therefore, the combination of metabolic profiling and gene expression abundance has been proven to be a powerful tool and has been successfully applied to determine the key metabolites and limiting steps [16].

In this study, GC–MS platform-based metabolomics was carried out to investigate intracellular metabolic difference between the wild-type and mutant strain. The pattern recognition methods of principal component analysis (PCA), partial least squares (PLS) and partial least squares-discriminant analysis (PLS-DA) were used to determine key biomarkers related to rapamycin production. Subsequently, metabolic pathway analysis using MetPA was performed to identify a key metabolic module associated with rapamycin synthesis. Then, exogenous feeding strategy was performed to further verify the results of metabolic profile analysis and identify the vital pathway for the improvement of rapamycin production. Finally, real-time PCR and enzyme activity assays were employed to comparatively analyze the impact of key enzymes on the rapamycin synthesis.

Materials and methods

Microorganism and culture condition

Wild-type ATCC 29253 of *S. hygroscopicus* used in this study was a stock of our laboratory and was cultivated on the agar slant medium about 12–15 days to harvest spores. Fresh slants were washed into 100 mL un-baffled shake flask containing glass beads with 3–5 mL sterile water, and it was shaken and filtered to acquire single spore suspension. An aliquot of 0.5 mL resulting single spore suspension (10^8/mL) was inoculated into a 250 mL un-baffled shake flask containing 30 mL seed medium, and incubated at 28 °C, 220 rpm for 60 h. Then, 3 mL seed cultures were transferred into a 250 mL un-baffled shake flask containing 30 mL fermentation medium, and cultured at 28 °C, 220 rpm for 120 h.

Slant and plate medium contained 4.0 g/L mannitol, 20 g/L oat, 2.5 g/L yeast extract, and 20 g/L agar, pH 7.0. The seed medium was composed of 20 g/L soluble starch, 20 g/L glucose, 10 g/L corn flour, 6 g/L peptone, 6 g/L yeast powder, 1.5 g/L casein hydrolysate, 0.25 g/L $MgSO_4{\cdot}7H_2O$ and 1.0 g/L K_2HPO_4 and pH 7.0. The fermentation medium contained 20 g/L glycerin, 20 g/L dextrin, 10 g/L soybean meal, 5.0 g/L peptone, 5.0 g/L yeast powder, 0.5 g/L K_2HPO_4, 0.5 g/L KH_2PO_4, 0.5 g/L NaCl, 2.0 g/L $MgSO_4{\cdot}7H_2O$ and 1.5 g/L L-lysine, and pH 6.5. In the process of medium preparation, soybean meal and corn flour in the medium were first dissolved quantitatively, autoclaved, and then centrifuged at 10,000×*g* for 10 min at 4 °C to remove the insoluble ingredients. After that, other medium compositions were quantitatively added into the supernatant of soybean meal and autoclaved again.

UV mutagenesis and mutants screening

The detailed UV mutagenesis was performed according to the methods described by Zhu et al. [50] with slight modifications. The single spore suspension of *S. hygroscopicus* ATCC 29253 was exposed to UV rays at a distance of 20 cm from UV lamp for 10, 20, 30, 50, 60, 80, and 100 s, subsequently incubated on the ice bath for 2 h. To avoid any photoreaction resulting in reverse mutation of strains, all procedures and exposures were carried out in a dark room. Then, the spore suspension was diluted and spread on agar plate medium and incubated at 28 °C for 6–7 days.

A high-throughput screening method was employed to acquire high-yielding strains [46]. Single colony from agar plate medium was transferred into one corresponding well of the duplicate 96-well plates (A and B) which were incubated at 28 °C for 10 days. Then, each medium in one 96-well plate (A) was plugged out and transferred

into 1.5 mL Eppendorf tube with 0.5 mL methanol, subsequently incubated at room temperature for 12 h. Methanol extracts were centrifuged and used for bioassay. Another 96-well plate (B) was stored at 4 °C for further fermentation according to results from 96-well plate A.

On the basis of the above procedure, the over-producing mutants were obtained. To test the genetic stability of rapamycin production ability, the high-yielding mutants were continuously sub-cultured for ten generations from agar slant medium to the next and each generation should be cultured under the same conditions.

Analytical methods of rapamycin production

The concentration of rapamycin was measured by HPLC method [48]. Briefly, 2 mL of culture samples was extracted and immediately mixed with 2 mL methanol, and then was shaken intermittently in a water bath at 50 °C for 120 min. The fermentation suspension was centrifuged at 8000×*g* for 10 min. The concentration of rapamycin in fermentation broth was determined by HPLC (Agilent 1200, USA) equipped with a Zorbax SB-C18 analytical column (250 mm × 4.6 mm; Agilent Technologies). The mobile phase was mixture of methanol, acetonitrile and water (70:15:15, v/v/v) with a flow rate of 1.0 mL/min, using UV detector at 277 nm, and the column temperature was 40 °C. The concentration of rapamycin in the samples was measured using a calibration curve generated by authentic rapamycin standards (MP Biomedicals, USA). Dry cell weight (DCW) was measured by sampling 5 mL cell cultures, the fermentation broth was centrifuged at 8000×*g* for 10 min and washed with sterile deionized water, then dried to a constant weight at 80 °C. Total sugar content was measured by phenol–sulfuric acid method [49] with glucose as a standard [19].

Sample preparation of intracellular metabolites for GC–MS

Samples' quenching and extraction of intracellular metabolites were performed according to the methods described by Wentzel et al. [41] with slight modifications. At each sampling time point (48, 72, 96 and 120 h), 10 mL of culture samples was taken from the fermentation vessel of the wild-type and mutant strain and immediately transferred to a 50 mL tube containing 40 mL 60 % cooled methanol solution pre-chilled on a methanol bath refrigerated at −40 °C. The whole procedure from sampling to quenching was completed within 10–15 s. The samples were mixed vigorously with a vortex mixer (HYQ-3110; Crystal Technology, USA) for 2 s, and stored at −40 °C for quenching about 5 min to stop cellular metabolism. The mixture was centrifuged at 8000×*g* for 10 min at −20 °C, the supernatant was removed while the cell pellet was washed at least three times with 10 mL 0.9 % (w/v) NaCl solution refrigerated at 4 °C, and subsequently was centrifuged at 5000×*g* for 5 min at 4 °C. The resulting cell pellet was grinded using liquid nitrogen for crushing cell wall and dissolved in the 1.5 mL tube containing 1.0 mL cooled methanol solution (50 % (v/v), −40 °C). The freeze–thaw cycle was repeated for at least three times, and then the cell extract was centrifuged at 10,000×*g* for 5 min at −20 °C. The supernatant was collected in the another 1.5 mL tube and additional 0.5 mL cold methanol–water solution [50 % (v/v), −40 °C] was added into cell pellet to completely extract the samples. The extracted cell pellet was re-suspended for 30 s and then centrifuged at 10,000×*g* for 15 min at −20 °C. The supernatant was collected and pooled with the former one, then stored at −80 °C.

Next, a 100-μL aliquot of sample extracts mixed with 20 μL succinic d4 acid (0.2 mg/mL) as the internal standard was lyophilized for 12 h (Alpha 1-2LD PLUS, Christ, Germany). After lyophilization, the samples were subjected to two-stage chemical derivatization with 50 mL methoxamine hydrochloride (20 mg/mL in pyridine) and incubated at 40 °C for 80 min. Subsequently, 80 mL *N*-methyl-*N*-(trimethylsilyl) trifluoroacetamide was added into the sample and incubated at 40 °C for 80 min for trimethylsilylation [22].

Determination of intracellular metabolites by GC–MS

The derivatized metabolite samples were detected and analyzed by GC–MS using an Agilent 6890N-5975C MSD system (Agilent Technologies, CA) equipped with a DB-5MS capillary column (30 m × 0.25 mm, 0.25 mm film thickness, Agilent Technologies, CA) and an Agilent 7683B auto-sampler. One microliter of the derivatized sample was injected with a split ratio of 1:1. Helium was used as the carrier gas at a flow rate of 1.0 mL/min. The column temperature was initially held at 70 °C for 2 min, then raised to 270 °C with a gradient of 8 °C/min and held for 3 min. The interface temperature was set at 250 °C; mass spectra were obtained from iron beam of 70 eV under an ionization current of 40 μA with a scan range of 50–650 *m*/*z*.

Extraction of total RNA

The whole RNA was isolated from *S. hygroscopicus* wild-type and mutant strain grown in fermentation medium at 72 h, when cell growth entered logarithmic phase according to method of Jung et al. [20]. The cell pellets were harvested by centrifugation and grinded using liquid nitrogen, and then suspended using 1 mL of Trizol reagent (Invitrigen™, USA) as an extracting solution (Sigma, USA),

subsequently incubated at room temperature for 5 min. The mixture was centrifuged at 12,000×*g* for 5 min at 4 °C. The supernatant was transferred into 200 μL of chloroform, vortex-mixed and followed by the incubation at room temperature for 5 min, centrifuged at 12,000×*g* for 15 min at 4 °C. The supernatant was transferred into a new tube and mixed with 400 μL isopropanol, vortex-mixed and followed by the incubation at room temperature for 10 min, centrifuged at 12,000×*g* for 10 min at 4 °C. The cell pellets were washed using 75 % alcohol, and centrifuged at 12,000×*g* for 5 min at 4 °C. After drying for 5 min, the pellets were dissolved using 20 μL DEPS-free water. To remove DNA mixed in RNA, DNase I (Fermentas, USA) was added into the RNA extraction, and treated for 1 min. The integrity of RNA was detected by means of formaldehyde denaturing agarose gel electrophoresis, and then the concentration and purity of RNA were measured on the basis of the optical absorbance ratio of RNA samples at 260 and 280 nm.

Gene transcription expression analysis of key enzymes by real-time RT-PCR

To supply accurate gene sequence for analysis of RT-PCR, the target genes of primary metabolism were amplified and sequenced with the primer designed on the basis of genomic sequence of *Streptomyces rapamycinicus* strain NRRL 5491 [1]. Then, real-time PCR was carried out to detect gene relative transcriptional expression abundance according to the method of Borges et al. [2]. cDNA was prepared using PrimeScript™ RT reagent Kit (Takara, Dalian, China) under instructions. Then, RT-PCR analysis of each gene was performed in a Bio-Rad iQ5 (Bio-Rad, USA) with the SYBR® Premix Ex Taq™ (Takara, Dalian, China) under the manufacturer's protocol. The house-keeping gene *hrdB* was regarded as internal standard to normalize abundance of target genes expression. The sequences of primers for quantitative real-time RT-PCR are listed in Table 1. The data of qRT-PCR were analyzed by $2^{-\Delta\Delta C_T}$ method [34].

Enzymes activity assays

Samples for enzyme activity analysis were harvested at 72 h when cell growth entered logarithmic phase. An aliquot of 10 mL fermentation broth was centrifuged at 10,000×*g* for 10 min at 4 °C. Cell pellets were washed three times by 100 mM Tris–HCl (pH 7.0) including 20 mM KCl, 5 mM $MnSO_4$, 2 mM DTT and 0.1 mM EDTA, and then re-suspended in the same buffer. Cell suspension was broken by ultra-sonication for 10 min (10 successive cycles with each cycle containing 30 s on and 30 s off), subsequently centrifuged at 12,000×*g* for 20 min. The resulting suspension was stored at −80 °C for further analysis of total protein concentration and enzyme activity.

Table 1 Sequences of primers for quantitative real-time RT-PCR

Primer name	Sequence (5′–3′)
pyc-RTF	GAGGCGATGAAGATGGAG
pyc-RTR	CTGCTGAATCGTGTTGATG
dapA-RTF	ACTCGCTGCTCATCTGGTG
dapA-RTR	TTCTCCGCATCGCTGGTG′
rapL-RTF	CTGCTGAATCGTGTTGATG
rapL-RTR	ATGGTGGGCAGGTTGAAGC
hrdB-RTF	GAACTTGTAGCCCTTGGTGTAG
hrdB-RTR	TGCTCTTCCTGGACCTCATC

We used Bradford method [42] to measure concentration of total protein. The pyruvate carboxylase (PCx, EC 6.4.1.1) activity was assayed by monitoring the decrease of NADH at 340 nm [30]. Activity of the dihydrodipicolinate synthase (DHDPS, EC 4.2.1.52) was measured using a coupled assay originally described by Sibarani et al. [36]. The activity of lysine cyclodeaminase (LCD, EC 4.3.1.28) was measured by the method of Tsotsou and Barbirato [40].

Data processing and multivariate statistical analysis

The integration and de-convolution of GC–MS data were carried out in the Mass Spectral De-convolution and Identification System, Version3.2 (National Institute of Standards and Technology, Gaithersburg, MD). The annotation of metabolites was performed via matching their mass fragmentation patterns with those in the NIST mass spectral library (2008, Gaithersburg, MD, USA) and the Golm Metabolome Database. The match factor was more than 50 %. According to retention time, all GC–MS data formed a matrix about the relative abundance of metabolites at different time.

The peak area of each metabolite was normalized to the internal standard succinic acid d_4 and cell biomass. The matrix generated from relative abundance of all metabolites identified was imported into SIMCA-P package (Ver 11.5; Umetrics, Umea, Sweden) as well as MATLAB and uploaded into web-based platform using MetaboAnalysis 3.0 (http://www.metaboanalyst.ca) [43, 44] for the multivariate statistical analysis. Each sample contained three biological replicates. The relative abundance of each metabolite, relative transcriptional abundance of genes and activity of each enzyme between the wild-type and mutant strain of *S. hygroscopicus* were analyzed using a Student's *t* test performed with SPSS 20.0 software package.

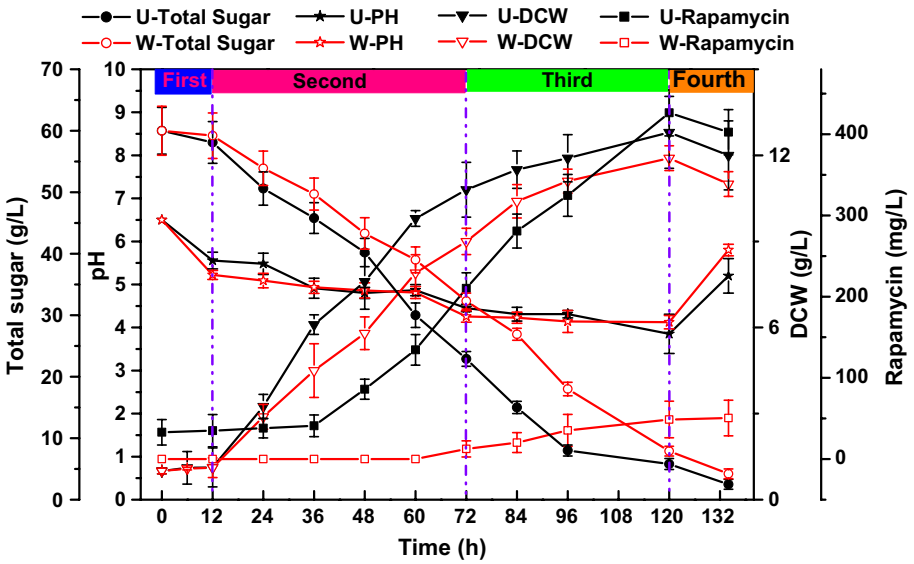

Fig. 1 Dynamic fermentation profiles of the dry cell weight, the total sugar, pH value, and rapamycin production between the wild-type and mutant strain under the same culture condition. *W* represents wild-type and *U* represents mutant. The *values* represent the means of five independent experiments and the *error bars* mean standard deviations of five values

Results

Comparison of fermentation kinetics between the wild-type and mutant strain

Fermentation characteristics were compared between the wild-type *S. hygroscopicus* ATCC 29253 and mutant *S. hygroscopicus* U2-3D9 under the same culture condition. As shown in Fig. 1, the whole fermentation process could be divided into four phases, namely lag phase (0–12 h), logarithmic phase (12–72 h), stable phase (72–120 h) and decline phase (120–134 h). In the lag phase, DCW reached 1.11 and 1.13 g/L in the wild-type and mutant strain of *S. hygroscopicus*, respectively. The pH value decreased to 5.6 and 5.2 from initial 6.5, due to some organic acid produced at this period (see Supplementary Table S1). However, rapamycin production was not detected in the wild-type strain and was only 35.1 mg/L in the mutant strain.

In the logarithmic phase (12–72 h), the total sugar in the medium sharply decreased to 22.9 and 32.3 g/L in the mutant and wild-type strain, respectively. The pH value kept at the range from 4.5 to 5. Cell growth rate of the mutant strain was 0.16 g/(L·h) and the highest cell biomass reached 10.8 g/L, while in the wild-type strain, cell growth rate was 0.13 g/(L·h) and the highest biomass was 9.0 g/L, indicating the mutant grew faster than the wild-type strain. It should be noted that the rapamycin production of the wild-type strain had only 12 mg/L at 72 h, while the production of rapamycin in the mutant strain started to increase from 35.1 to 210.2 mg/L. One probable explanation was that accumulation of secondary metabolites was a response to the external environment that was not in favor of cell growth, when an organism was growing at its full potential [24].

In the stable phase (72–120 h), when rapamycin began accumulating in large quantities, the production of rapamycin sharply increased from 210.2 to 426.7 mg/L. Thus, the highest production of rapamycin was achieved at 120 h, which was approximately 5.8-fold compared to that of the wild-type strain (from 12 to 48.7 mg/L). Besides, the pH varied from 3.9 to 4.5. However, the pH value of the mutant and wild-type strain suddenly increased to 5.2 and 5.8 after 120 h, while rapamycin production began to decrease. It is speculated that it might be due to an effect of organic acids' consumption [45]. And previous research has reported that a weak alkaline final pH value was unfavorable for the accumulation of rapamycin [25].

Determination of key biomarkers and metabolic module closely associated with rapamycin biosynthesis by comparative metabolomics

Fermentation characteristics supplied the extracellular cues for cell growth and rapamycin production. However, the mechanism of rapamycin overproduction discrepancy was not still understood. To solve this, the analysis of intracellular metabolic profile was carried out by GC–MS to reveal key biomarkers and metabolic module as well as key enzymes in rapamycin overproduction. Samples were obtained from the wild-type strain and mutant strain U2-3D9 to detect the pools of intracellular metabolites every 24 h (48, 72, 96 and 120 h). Three parallel experiments were performed at each time point. As a result, about 86 metabolites were identified and quantified by GS-MS (Supplementary Table S1), including 29 organic acids, 25 amino acids and amides, 10 sugars and alcohols, 8 fatty acids, 7 nucleotides and 8 other compounds.

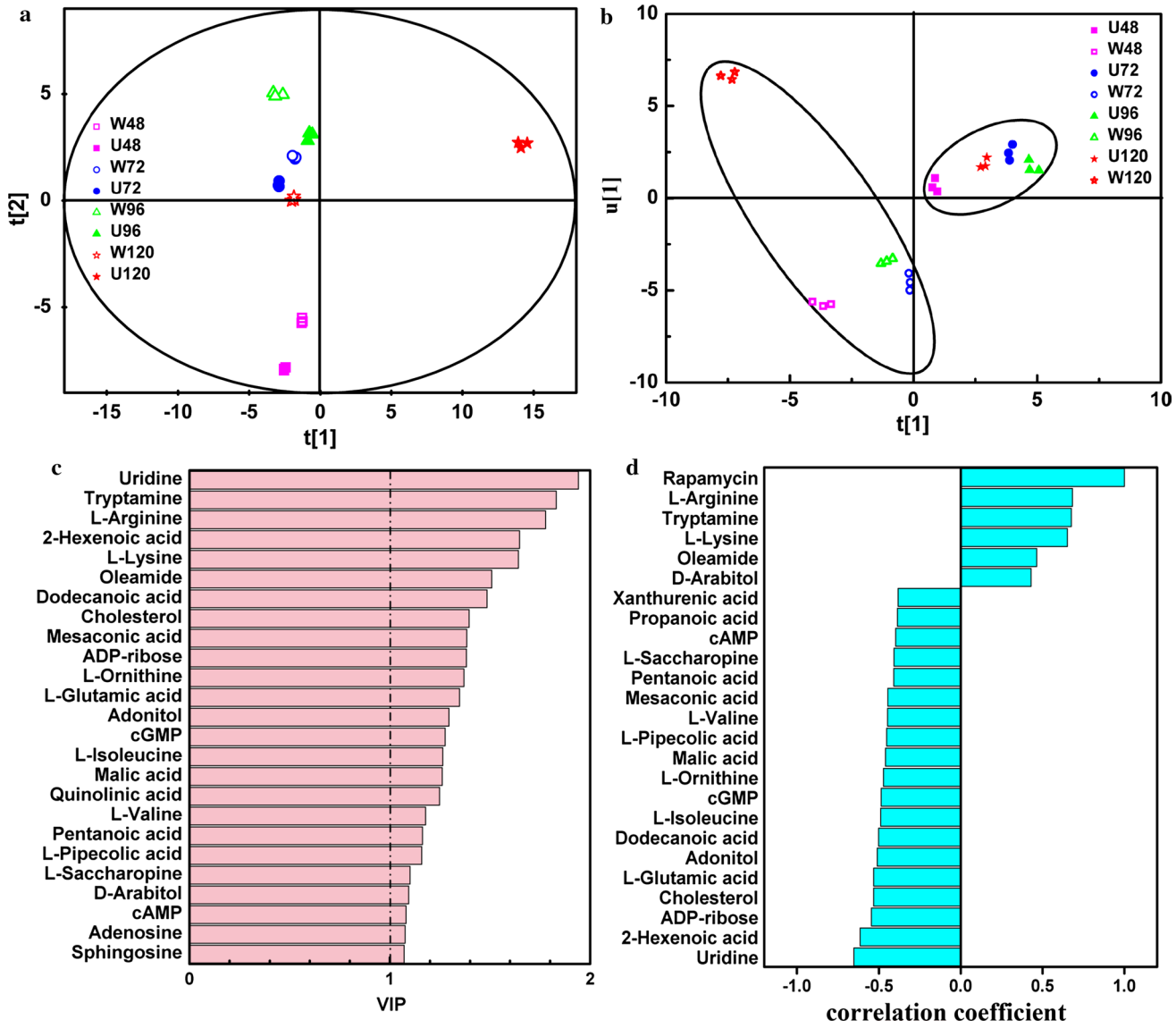

Fig. 2 PCA, PLS and PLS-DA analysis of intracellular metabolites from the wild-type and mutant strain. The samples were withdrawn from the cultivation at 48, 72, 96 and 120 h. **a** PCA-derived score plots; **b** PLS-derived score plots; **c** PLS-derived loading plots; **d** 25 compounds correlated with the rapamycin by PLS-DA. *W* represents wild-type strain, *U* represents mutant strain

Next, PCA ($R^2 = 0.971$, $Q^2 = 0.913$) and hierarchical clustering algorithm were performed to analyze structure and quality of metabolomics data. In the score plot (Fig. 2a), the tight clustering of three parallel samples at each time point and clear separation between the samples of the two strains indicated that these data were suitable for further analysis of different metabolic characteristics and monitoring culture process at different phases [9]. Heat map combined with the hierarchical clustering analysis reconfirmed the above conclusion (Fig. 3). Simultaneously, PLS (using rapamycin yield as *Y* value, R^2 $(X) = 0.594$, R^2 $(Y) = 0.91$, $Q^2 = 0.789$) was performed to analyze samples from different strains and culture phases. In the score plot (Fig. 2b), the samples from the mutant strain were located in the first quadrant of the coordinate axes owing to relative higher rapamycin production. In contrast, another samples from the wild-type strain mainly gathered in the lower left corner of the coordinate system. PLS analysis was consistent with PCA and Hierarchical clustering algorithm, suggesting the rationality of sample extraction and the reliability of data.

Moreover, PLS analysis was applied to evaluate the correlation of metabolites to rapamycin production. Accordingly, the variable importance of the projection plots (VIP) on each metabolite was generated by PLS (Fig. 2c). VIP value indicated the contribution of each metabolite to the

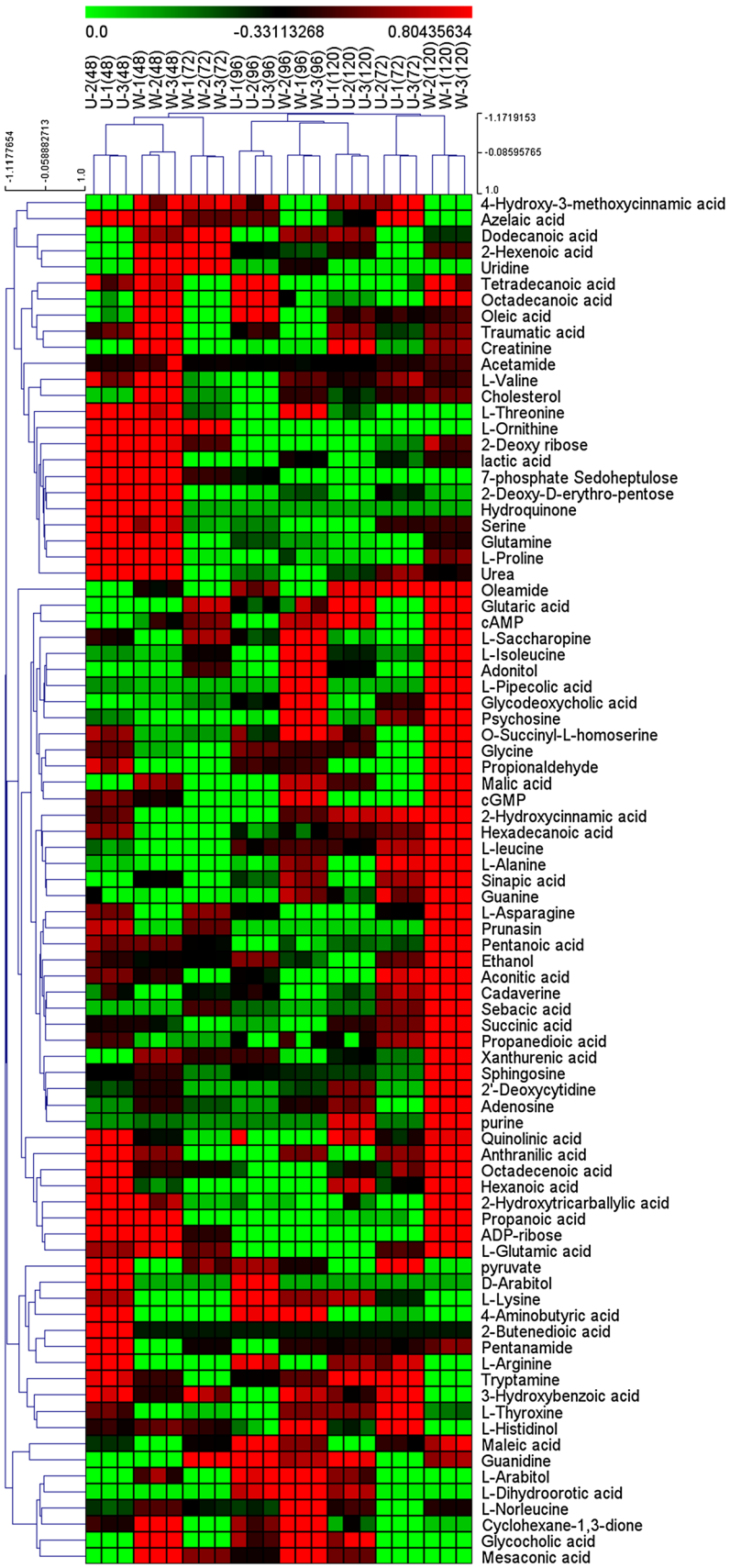

Fig. 3 Hierarchical clustering algorithm of all samples, *different colors* represent distinct relative abundance of metabolites, replicate samples cluster together, and samples from different strains and time points are separated with each other. Relative abundance of intracellular metabolites has been changed in the times courses (color figure online)

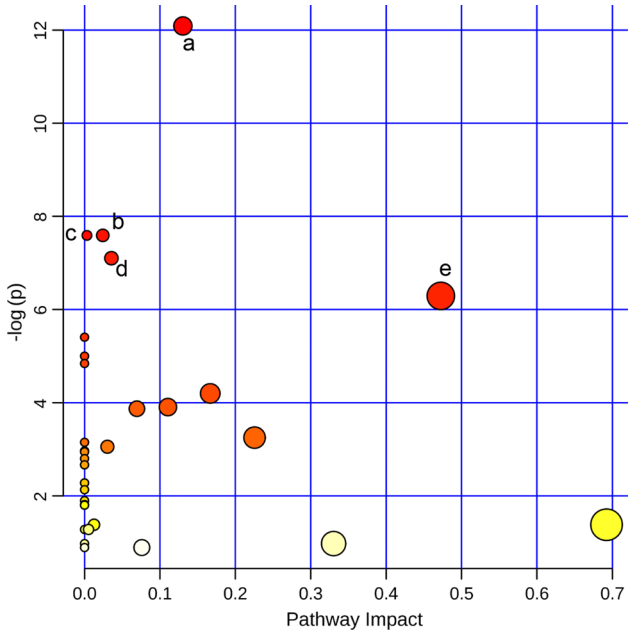

Fig. 4 Metabolic pathway analysis, the 'metabolome view' shows all matched pathways according to *p* values by pathway enrichment analysis and pathway impact values by pathway topology analysis. *a* Aminoacyl-tRNA biosynthesis ($p = 5.6 \times e^{-6}$); *b* phenylalanine metabolism ($p = 0.0005$); *c* pantothenate and CoA biosynthesis ($p = 0.0005$); *d* valine, leucine and isoleucine biosynthesis ($p = 0.0008$); *e* glycine, serine and threonine metabolism ($p = 0.0019$)

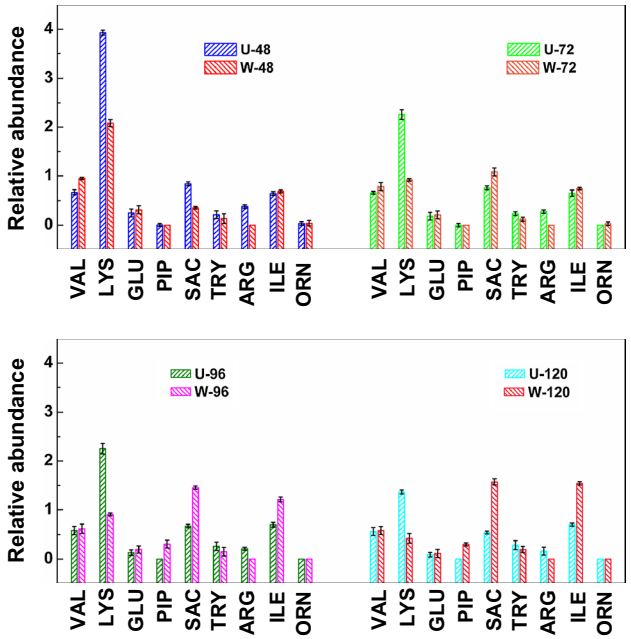

Fig. 5 Dynamically comparative analysis of amino acids metabolic modules between the wild-type and mutant strain at 48, 72, 96 and 120 h. *VAL* valine; *LYS* lysine; *GLU* glutamate; *PIP* pipecolic acid; *SAC* saccharopine; *TRY* tryptamine; *ARG* arginine; *ILE* isoleucine; *ORN* ornithine

synthesis of rapamycin. A total of 25 metabolites (VIP score >1) ranked in the top were chosen as candidate biomarkers. Meanwhile, 25 metabolites associated with rapamycin production were also found by PLS-DA according to correlation coefficient (Fig. 2d). Among them, 19 metabolites were positively correlated with rapamycin production, while the rest had negative correlation with rapamycin production. Ultimately, it was concluded that 22 metabolites in the analysis of PLS-DA were the same as that in the analysis of PLS (Supplementary Table S2).

To further analyze the most relevant metabolic pathway of rapamycin synthesis, MetPA integrated with KEGG pathway database was performed on the basis of 22 metabolites (see Supplementary Table S2) derived from the above analysis. The 'metabolome view' shows all matched pathways according to *p* values by pathway enrichment analysis and pathway impact values by pathway topology analysis. In Fig. 4, *Y*-axis means the minus logarithm of *p* value calculated from the pathway enrichment analysis, and *X*-axis represents the impact value calculated from pathway topology analysis. The *p* values of aminoacyl-tRNA biosynthesis ($p = 5.6 \times e^{-6}$), phenylalanine metabolism ($p = 0.0005$), pantothenate and CoA biosynthesis ($p = 0.0005$), valine, leucine and isoleucine biosynthesis ($p = 0.0008$) and glycine, serine and threonine metabolism ($p = 0.0019$) were <0.01 (see Supplementary Table S3), indicating their close correlation with rapamycin synthesis. Therefore, amino acid metabolism might be a key metabolic module of rapamycin synthesis.

Analysis of amino acid metabolic module and key biomarkers for potential regulation of rapamycin overproduction

Significant differences in the abundances of intracellular amino acids were observed between the wild-type and mutant strain. In fact, amino acids are essential parts of carbon and nitrogen metabolism for maintaining cell growth and protein synthesis. In addition, amino acid catabolism is a vital source of fatty acid precursors [39] for rapamycin biosynthesis [37]. The pools of intracellular metabolites in amino acid metabolic module containing valine, isoleucine, glutamate, arginine, ornithine, tryptamine, lysine, pipecolic acid, and saccharopine (VIP score >1 and those closely associated with rapamycin production) were compared between the wild-type and mutant strain during the fermentation period in detail, as shown in Fig. 5.

Valine and isoleucine metabolism

Relative abundance of valine at four time points (48, 72, 96 and 120 h) in the mutant was much lower than that of the

wild-type strain (Fig. 5). Meanwhile, a clear negative correlation could be observed between concentrations of valine and rapamycin production, as shown in Fig. 2d. Relative abundance of isoleucine in the mutant strain was 0.646, 0.651, 0.698, 0.701, respectively, and a little lower than that in the wild-type strain. When cell growth entered into the stable phase, the metabolic difference between the mutant and wild-type became more obvious, and relative level of isoleucine in the wild-type strain was about twofold of that in the mutant strain. In fact, both isoleucine and valine are the precursors of methylmalonyl-CoA [21, 23], which is a key node of the carbon flux, switching from the primary metabolism into the secondary metabolic branch [28, 32]. Therefore, more isoleucine and valine in the mutant strain might supply methylmalonyl-CoA for rapamycin synthesis. As analyzed above, methylmalonyl-CoA is a key node for improving rapamycin production, while valine and isoleucine metabolism are key metabolic modules related to rapamycin synthesis. This conclusion was consistent with the reports by Jung et al. [20] and Cheng et al. [6].

Glutamate, arginine and ornithine metabolism

VIP values of glutamate, arginine and ornithine were 1.3, 1.8 and 1.4, respectively, indicating their close association with rapamycin production. In Fig. 4, the relative abundance of glutamate in the mutant strain was 0.25 (48 h), 0.18 (72 h), 0.13 (96 h), 0.09 (120 h), while that of the wild-type strain was 0.31, 0.21, 0.19, 0.11. Along with cell growth, the relative level of glutamate began to decrease, but during the whole fermentation period, relative abundance of glutamate in the wild-type strain was always higher than that in the mutant strain.

Relative level of arginine in the mutant strain was 0.38 (48 h), 0.28 (72 h), 0.21 (96 h) and 0.16 (120 h), while arginine was not detected in the wild-type strain. Ornithine in the mutant strain reached its peak of 0.0328 at 48 h in Fig. 5, but it cannot be detected at other time points. In the wild-type strain, relative abundance of ornithine was 0.04 (48 h), 0.0296 (72 h) and was not detected at the other two time points. As we all known, arginine and ornithine are involved in urea cycle [29]. Thus, in the mutant strain, more arginine might be metabolized into urea. Additionally, it might be speculated that urea cycle might be a potential key metabolic module to provide a nitrogen source for rapamycin synthesis.

Tryptophan metabolism

The relative abundance of tryptamine in the mutant strain was approximately 50 % higher than that in the wild-type strain in the whole fermentation period. Tryptamine is an intermediate metabolite related to shikimate metabolic pathway which generates chorismate by the chorismate mutase. Ultimately, chorismate metabolism provides a starting unit (4R,5R)-4,5-dihydroxycyclohex-1-enecarboxylic acid (DHCHC) for rapamycin synthesis [15, 33]. In that case, the depletion of intracellular tryptophan or the high level of tryptamine might indicate the strong activeness of shikimate metabolic pathway, leading to generate more DHCHC for rapamycin synthesis. On the other hand, high intracellular abundance of aromatic amino acids may influence other metabolic reactions. For example, as the rate-limiting step in shikimate synthesis originating from erythrose 4-phosphate and phosphoenolpyruvate, 3-deoxy-7-phosphoheptulosonate synthase could be inhibited due to high intracellular abundance of aromatic amino acids [45].

Lysine metabolism

The relative level of intracellular lysine in the mutant strain was 3.92 (48 h), 2.25 (72 h), 2.25 (96 h) and 1.36 (120 h), and the relative abundance of the wild-type strain was 2.08, 0.92, 0.91 and 0.42, respectively. It could be seen that more lysine was quickly consumed in the mutant strain to synthesize rapamycin from 48 to 120 h. However, the intracellular concentration of lysine was higher in the mutant strain compared to the wild-type strain, indicating that lysine plays an important role in rapamycin overproduction. In addition, the relative levels of both saccharopine and pipecolic acid in the mutant were lower than those in the wild-type strain. Along with the fermentation process, intracellular concentrations of the two metabolites involved in amino acids metabolism were continuously declined both in the mutant and wild-type strain.

In sum, more amino acids were used to supply precursors for rapamycin synthesis in the mutant strain, compared to that in the wild-type. As shown in Fig. 2c, these amino acids were the main contributors to differences of rapamycin production and fermentation performance. In addition, the result indicated the shortage of valine, glutamate, isoleucine, and ornithine in the synthesis of rapamycin (Fig. 2d). But lysine and rapamycin production was positively correlated since its coefficient was greater than zero, implying that the addition of lysine to the fermentation medium might help improve the supply of intracellular lysine in the process of rapamycin synthesis. As described above, it was concluded that amino acid metabolism, including lysine and arginine, valine, glutamate, isoleucine and ornithine, is key for rapamycin synthesis.

Strengthening the relationship between intracellular amino acids and rapamycin synthesis

To confirm the above analysis, an exogenous feeding strategy was implemented by supplementing 2.5 g/L arginine,

tryptophan, lysine, glutamate, isoleucine, valine and ornithine into the fermentation medium at different culture phases [6, 27]. The result showed that rapamycin production was improved to different levels, as shown in Fig. 6. Addition of lysine and isoleucine at 24 h resulted in 2.3 and twofold increase of rapamycin concentration, respectively. Besides, rapamycin production was, respectively, improved by 1.7 and 1.3-fold after adding arginine and tryptophan at 36 h. Addition of ornithine at 60 h led to an improvement of rapamycin by 49.8 %. As the addition of valine and glutamate at 48 h, rapamycin production was increased to 265.3 and 231.5 mg/L, respectively. On the basis of the above effects on the rapamycin production after fed-batch of amino acids, the combinational addition of lysine, arginine and isoleucine was performed at different culture phases. Ultimately, rapamycin production of the mutant increased by 2.4-fold from 187.2 to 451.0 mg/L at 48 h. These results indicate that the addition of seven different amino acids was able to promote rapamycin production in varying degrees, and it was notable that addition of lysine resulted in the most significant improvement among other six amino acids and the simultaneous addition of these three amino acids (lysine, arginine and isoleucine) had synergistic effect on the production of rapamycin. Thereby, it was confirmed that amino acid metabolic module was closely associated with rapamycin synthesis indeed and the closest correlation was observed between lysine and rapamycin production.

Comparative analysis of gene transcription and key enzyme activities related to the lysine metabolic pathway

When entering into logarithmic phase (72 h), total RNA and proteins were extracted from the wild-type and mutant strain for transcriptional analysis and key enzyme activity measurements, respectively. As shown in Fig. 7a, the transcriptional level of the gene *dapA* encoding DHDPS was improved by 5.98-fold in the mutant strain compared to the wild-type strain. The relative transcriptional abundance of the gene *pyc* encoding PCx was 2.55 in the mutant strain, which increased by 2.93-fold over that in the wild-type strain. The relative transcriptional level of the gene *rapL* encoding LCD in the mutant strain (0.56) was about 1.34-fold improvement on the basis of that in the wild-type strain (0.14). Meanwhile, in Fig. 7b, the activities of PCx, DHDPS and LCD increased by 39.6, 53.2 and 36.4 % in the mutant strain, respectively. As a result, these three enzymes were not only increased by different extents, but also the enzymes activities were improved significantly in the mutant strain, suggesting that more metabolic flux of lysine might flow towards rapamycin synthesis in the mutant strain. Higher transcriptional levels and activities of key enzymes led to rapid consumption of primary metabolites

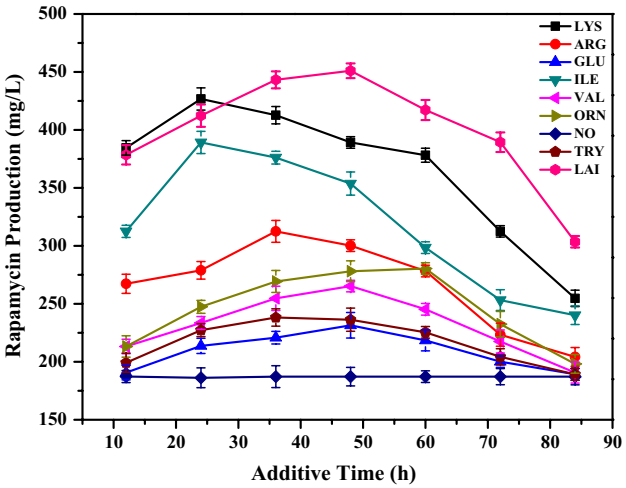

Fig. 6 The effect of rational feeding of amino acids on the rapamycin production. The *values* represent the means of five independent experiments and the *error bars* represent standard deviations. *NO* without any addition; *LYS* lysine; *ARG* arginine; *GLU* glutamate; *ILE* isoleucine; *VAL* valine; *ORN* ornithine; *TRY* tryptophan; *LAI* lysine, arginine and isoleucine

for rapamycin biosynthesis. This result could not only account for the metabolic difference between the wild-type and mutant strain, but also indicate that DHDPS played a vital role in rapamycin production due to the upregulated *dapA* as well as the significant increase of DHDPS activity.

Discussion

In the recent years, metabolomics has been increasingly applied in the industrial strains to trace cellular metabolic pathway and reveal underlying cellular metabolic mechanism. For example, comparative metabolomics based on GC–MS was employed to investigate the external stress mechanism in *Saccharomyces cerevisiae* under high cell density culture [11]. In this study, metabolomics enables us to gain comprehensive insights into complex cellular metabolic mechanisms in the synthesis of rapamycin. We used comparative metabolomics to analyze the metabolic difference between the wild-type ATCC 29253 and the mutant strain U2-3D9. The results showed that the amino acid metabolic module was very important for rapamycin synthesis. With PLS and PLS-DA, a total of 22 metabolites were identified as key biomarkers responsible for the discrimination of metabolic status between the wild-type and mutant strain and closely associated with rapamycin production. The complex metabolic network relationships in the cell as well as rapamycin biosynthesis are summarized in Fig. 8. It is observed that the precursors of rapamycin synthesis are provided directly or indirectly by these metabolic pathways. Besides, intracellular metabolic network

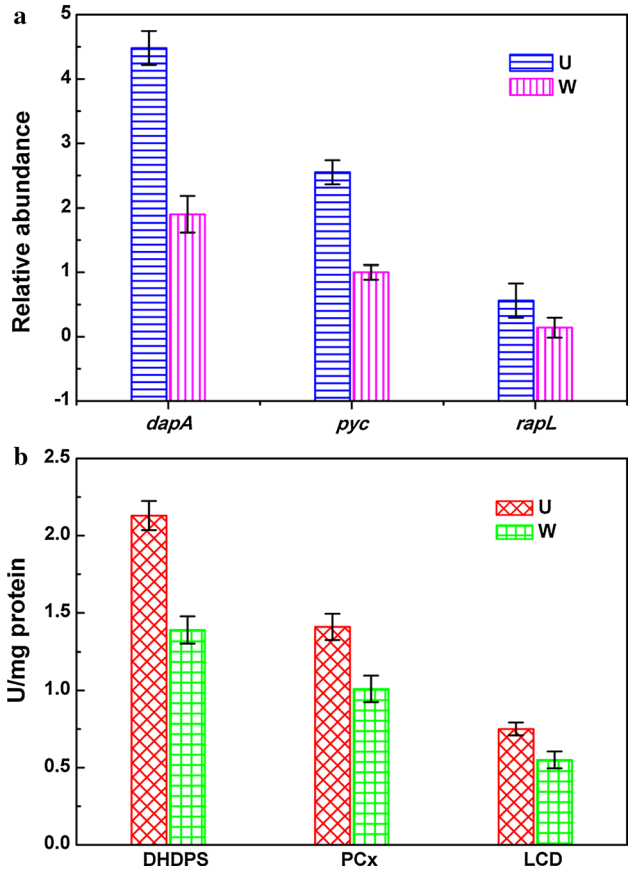

Fig. 7 Comparative analysis of key genes expression and key enzymes activities. **a** Transcriptional levels of the genes *dapA*, *pyc*, *rapL* between the wild-type and mutant strain; **b** key enzymes activities of lysine pathway between the wild-type and mutant strain. *Each value* represents the average of three independent experiments and the *error bars* represent standard deviations. *DHDPS* dihydrodipicolinate synthase; *PCx* pyruvate carboxylase; *LCD* lysine cyclodeaminase

is composed of a variety of metabolic modules, which are influenced and interact with each other.

As described above, amino acid metabolic module was discovered as a key metabolic module related to rapamycin synthesis using MetPA pathway analysis, demonstrating that amino acid metabolism plays a crucial role in the process of rapamycin production. Besides, the previous research has reported that the degradation of proteins might be beneficial for cell in response to external pressure [10], which demonstrated that the intracellular amino acid metabolism was crucial for maintaining normal cell life activities. Therefore, amino acid metabolism not only generates the precursors and nutrition for rapamycin synthesis, but also occupies a very important position in maintaining cell life activities among the entire metabolic networks.

By dynamically comparing differences in amino acid metabolic module between the mutant and wild-type stains, it was concluded that amino acids of the mutant strain were efficiently consumed and used to synthesize more rapamycin, resulting in a shortage for the mutant strain, namely "nitrogen starvation". The difference of amino acid module between the mutant and wild-type strain might originate from many reasons. One is probably associated with the availability of different precursors, owing to the fact that amino acid metabolism is closely related to glycolysis and tricarboxylic acid (TCA) cycle (Fig. 8). Another is the indispensable energy metabolism, where the TCA cycle and the glycolysis are the two main energy supply stations for cell life activities in primary metabolism. However, this research indicated that more amino acids were metabolized to synthesize more rapamycin. Furthermore, amino acids are also a vital source of CoA-ester precursors during rapamycin biosynthesis, especially valine, proline, leucine, isoleucine and threonine. According to Dotzlaf et al. [12], amino acids mainly participate in the following three metabolic modules: module I offers propionyl-CoA by oxidative process; module II is involved in the TCA cycle; and module III can be catalyzed and generated to acetoacetyl-CoA. Actually, these three main intracellular metabolic modules are mutually interrelated and cooperated to regulate the cellular complex metabolic events. By adding different amino acids, it was also indicated that changes of the intracellular amino acids generated a significant impact on synthesis of rapamycin, which was consistent with previous report [6, 38]. Actually, except for the contribution of amino acids to rapamycin synthesis, the effects of (2S)-malonayl-CoA and (2S)-methylmalonyl-CoA on rapamycin production have been researched and reported by Jung et al. [20] and they were the two main contributors of rapamycin synthesis.

As a rate-limiting step, DHDPS catalyzes the first committed reaction of L-lysine biosynthesis [14]. The metabolic flux of the rate-limiting step might be significantly increased owing to enhancement of DHDPS activity, which could make cell accumulate more lysine for rapamycin synthesis [18]. PCx, an anaplerotic enzyme, has been proven to be a major bottleneck for lysine production in *Corynebacterium glutamicum* [31]. The improvement of enzyme activity also helps to increase intracellular availability of the lysine. Additionally, by increasing influx of the oxaloacetate, metabolic module of TCA cycle is also improved. It is known that pipecolic acid is generated from lysine metabolism under the catalysis of LCD [17]. Thereby, sufficient precursors and nutrition are quite necessary for rapamycin synthesis. Therefore, these three enzymes played a pivotal role in the synthesis of rapamycin in terms of transcription and enzyme activity. It was obvious that DHDPS exhibited the most significant improvement in the mutant strain by transcriptional analysis and enzyme activity determination, compared to the wild-type strain. Simultaneously, the feeding of asparagine could improve rapamycin production [6], indirectly demonstrating that the step reaction is

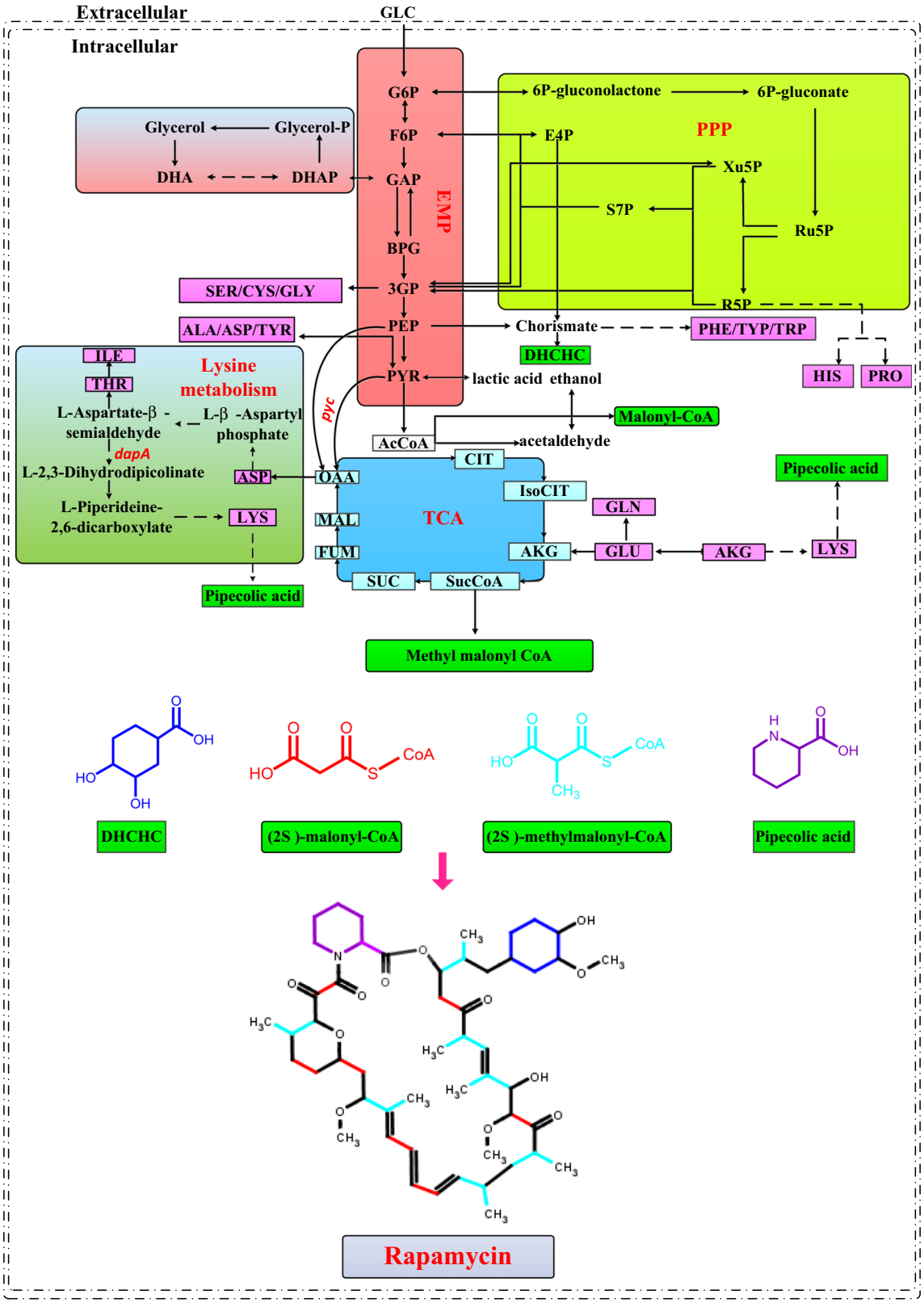

considerably important for rapamycin synthesis. Due to the increase in transcriptional expression and enzyme activities of DHDPS and PCx, the lysine metabolic reaction rate might be increased, ensuring sufficient supply of intracellular lysine. Additionally, the improvement of LCD can promote the conversion of pipecolic acid to rapamycin.

◀**Fig. 8** Schematic diagram of the proposed metabolic pathways closely associated with rapamycin biosynthesis in *S. hygroscopicus*. The key metabolic pathways are marked by *different colors*. *GLC* glucose; *G6P* 6-phospho-gluconate; *F6P* fructose-6-phosphate; *GAP* glyceraldehyde-3-phosphate; *DHAP* dihydroxyacetone phosphate; *DHA* dihydroxyacetone; *3GP* 3-phosphoglycerate; *PEP* phosphoenolpyruvate; *PYR* pyruvate; *AcCoA* acetyl-CoA; *CIT* citrate; *IsoCIT* isocitrate; *AKG* 2-oxoglutarate; *SucCoA* succiny-CoA; *SUC* succinate; *FUM* fumarate; *MAL* malic acid; *OAA* oxaloacetate; *E4P* erythrose-4-phosphate; *S7P* sedoheptulose-7-phosphate; *R5P* ribose-5-phosphate; *Ru5P* ribulose-5-phosphate; *Xu5P* xylulose-5-phosphate; *ALA* alanine; *ARG* arginine; *ASP* aspartate; *CYS* cysteine; *GLN* glutamine; *GLU* glutamate; *GLY* glycine; *HIS* histidine; *ILE* isoleucine; *LEU* leucine; *LYS* lysine; *PHE* phenylalanine; *PRO* proline; *SER* serine; *THR* threonine; *TRP* tryptophan; *TYR* tyrosine; *VAL* valine; *DHCHC* (4R,5R)-4,5-dihydroxycyclohex-1-enecarboxylic acid (color figure online)

These conclusions will provide some theoretical basis for the overproduction of rapamycin in the late stage.

To sum up, the comparative analysis of metabolic profiling coupling with RT-PCR and enzyme activity assays is a powerful tool for exploring major bottleneck of rapamycin synthesis and enables us to gain profound insights into global metabolic profiling. A straightforward approach of rational feeding strategy was used to relieve the problem of "nitrogen starvation" in the mutant strain. Actually, when lysine was supplemented into fermentation medium, rapamycin production showed a maximum improvement and increased to 426.7 mg/L from 187.2 mg/L by 2.3-fold. Subsequently, the simultaneous addition of amino acids had a superimposed effect on the rapamycin production. Ultimately, it was observed that amino acid metabolic module was a key module of rapamycin synthesis, especially lysine metabolism. Thus, RT-PCR and enzymes activities of lysine metabolic pathway could be applied to investigate the effects of key steps on rapamycin production. These three enzymes (PCx, DHDPS and LCD) involved in lysine metabolism were positively associated with rapamycin production, and it was indicated that DHDPS played a vital role in the synthesis of rapamycin. This work provides a theoretical basis to further improve rapamycin production and this rational solution can be applied in other research in the near future.

Acknowledgments This work was financially supported by the National 973 Project of China (No. 2013CB733600), the National 863 Project of China (No. 2011AA02A206), the Key Program of National Natural Science Foundation of China (No. 21236005), Specialized Research Fund for the Doctoral Program of Higher Education (No. 20110032130005) and the National Natural Science Foundation of China (No. 21176181).

References

1. Baranasic D, Gacesa R, Starcevic A, Zucko J, Blazic M, Horvat M, Gjuracic K, Fujs S, Hranueli D, Kosec G, Cullum J, Petkovic H (2013) Draft genome sequence of *Streptomyces rapamycinicus* strain NRRL 5491, the producer of the immunosuppressant rapamycin. Genome Announc 1(4). doi:10.1128/genomeA.00581-13
2. Borges AF, Fonseca C, Ferreira RB, Lourenco AM, Monteiro S (2014) Reference gene validation for quantitative RT-PCR during biotic and abiotic stresses in *Vitis vinifera*. Plos One 9(10). doi:10.1371/journal.pone.0111399
3. Calne RY, Collier DS, Lim S, Pollard SG, Samaan A, White DJ, Thiru S (1989) Rapamycin for immunosuppression in organ allografting. Lancet 2(8656):227
4. Chen SH, Hwang DR, Chen GH, Hsu NS, Wu YT, Li TL, Wong CH (2012) Engineering transaldolase in *Pichia stipitis* to improve bioethanol production. ACS Chem Biol 7(3):481–486. doi:10.1021/cb200396b
5. Chen X, Wei P, Fan L, Yang D, Zhu X, Shen W, Xu Z, Cen P (2009) Generation of high-yield rapamycin-producing strains through protoplasts-related techniques. Appl Microbiol Biotechnol 83(3):507–512. doi:10.1007/s00253-009-1918-7
6. Cheng YR, Fang A, Demain AL (1995) Effect of amino acids on rapamycin biosynthesis by *Streptomyces hygroscopicus*. Appl Microbiol Biotechnol 43(6):1096–1098
7. Cheng YR, Hauck L, Demain AL (1995) Phosphate, ammonium, magnesium and iron nutrition of *Streptomyces hygroscopicus* with respect to rapamycin biosynthesis. J Ind Microbiol 14(5):424–427. doi:10.1007/bf01569962
8. Cheng YR, Huang J, Qiang H, Lin WL, Demain AL (2001) Mutagenesis of the rapamycin producer *Streptomyces hygroscopicus* FC904. J Antibiot 54(11):967–972
9. Dietmair S, Hodson MP, Quek L-E, Timmins NE, Chrysanthopoulos P, Jacob SS, Gray P, Nielsen LK (2012) Metabolite profiling of CHO cells with different growth characteristics. Biotechnol Bioeng 109(6):1404–1414. doi:10.1002/bit.24496
10. Ding M-Z, Wang X, Yang Y, Yuan Y-J (2012) Comparative metabolic profiling of parental and inhibitors-tolerant yeasts during lignocellulosic ethanol fermentation. Metabolomics 8(2):232–243. doi:10.1007/s11306-011-0303-6
11. Ding MZ, Tian HC, Cheng JS, Yuan YJ (2009) Inoculum size-dependent interactive regulation of metabolism and stress response of *Saccharomyces cerevisiae* revealed by comparative metabolomics. J Biotechnol 144(4):279–286. doi:10.1016/j.jbiotec.2009.09.020
12. Dotzlaf JE, Metzger LS, Foglesong MA (1984) Incorporation of amino acid-derived carbon into tylactone by *Streptomyces fradiae* GS14. Antimicrob Agents Chemother 25(2):216–220
13. Douros J, Suffness M (1981) New antitumor substances of natural origin. Cancer Treat Rev 8(1):63–87. doi:10.1016/s0305-7372(81)80006-0
14. Eggeling L, Oberle S, Sahm H (1998) Improved L-lysine yield with *Corynebacterium glutamicum*: use of *dapA* resulting in increased flux combined with growth limitation. Appl Microbiol Biotechnol 49(1):24–30
15. Fang A, Demain AL (1995) Exogenous shikimic acid stimulates rapamycin biosynthesis in *Streptomyces hygroscopicus*. Folia Microbiol 40(6):607–610. doi:10.1007/bf02818516
16. Fridman E, Pichersky E (2005) Metabolomics, genomics, proteomics, and the identification of enzymes and their substrates and products. Curr Opin Plant Biol 8(3):242–248. doi:10.1016/j.pbi.2005.03.004
17. Gatto GJ, Boyne MT, Kelleher NL, Walsh CT (2006) Biosynthesis of pipecolic acid by RapL, a lysine cyclodeaminase encoded in the rapamycin gene cluster. J Am Chem Soc 128(11):3838–3847. doi:10.1021/ja0587603
18. Geng F, Chen Z, Zheng P, Sun J, Zeng A-P (2013) Exploring the allosteric mechanism of dihydrodipicolinate synthase by reverse engineering of the allosteric inhibitor binding sites and

its application for lysine production. Appl Microbiol Biotechnol 97(5):1963–1971. doi:10.1007/s00253-012-4062-8
19. Jeong E, Kim H-W, Nam J-Y, Shin H-S (2010) Enhancement of bioenergy production and effluent quality by integrating optimized acidification with submerged anaerobic membrane bioreactor. Bioresour Technol 101(Suppl 1):S7–S12. doi:10.1016/j.biortech.2009.04.064
20. Jung WS, Yoo YJ, Park JW, Park SR, Han AR, Ban YH, Kim EJ, Kim E, Yoon YJ (2011) A combined approach of classical mutagenesis and rational metabolic engineering improves rapamycin biosynthesis and provides insights into methylmalonyl-CoA precursor supply pathway in *Streptomyces hygroscopicus* ATCC 29253. Appl Microbiol Biotechnol 91(5):1389–1397. doi:10.1007/s00253-011-3348-6
21. Kamoun P (1992) Valine is a precursor of propionyl-CoA. Trends Biochem Sci 17(5):175–176. doi:10.1016/0968-0004(92)90258-b
22. Kassama Y, Xu Y, Dunn WB, Geukens N, Anne J, Goodacre R (2010) Assessment of adaptive focused acoustics versus manual vortex/freeze–thaw for intracellular metabolite extraction from *Streptomyces lividans* producing recombinant proteins using GC–MS and multi-block principal component analysis. Analyst 135(5):934–942. doi:10.1039/b918163f
23. Kasumov T, Martini WZ, Reszko AE, Bian F, Pierce BA, David F, Roe CR, Brunengraber H (2002) Assay of the concentration and C-13 isotopic enrichment of propionyl-CoA, methylmalonyl-CoA, and succinyl-CoA by gas chromatography–mass spectrometry. Anal Biochem 305(1):90–96. doi:10.1006/abio.2002.5639
24. Kim CJ, Chang YK, Chun GT (2000) Enhancement of kasugamycin production by pH shock in batch cultures of *Streptomyces kasugaensis*. Biotechnol Prog 16(4):548–552. doi:10.1021/bp000038f
25. Kim YH, Park BS, Bhatia SK, Seo HM, Jeon JM, Kim HJ, Yi DH, Lee JH, Choi KY, Park HY, Kim YG, Yang YH (2014) Production of rapamycin in *Streptomyces hygroscopicus* from glycerol-based media optimized by systemic methodology. J Microbiol Biotechnol 24(10):1319–1326
26. Kojima I, Cheng YR, Mohan V, Demain AL (1995) Carbon source nutrition of rapamycin biosynthesis in *Streptomyces hygroscopicus*. J Ind Microbiol 14(6):436–439. doi:10.1007/bf01573954
27. Lee MS, Kojima I, Demain AL (1997) Effect of nitrogen source on biosynthesis of rapamycin by *Streptomyces hygroscopicus*. J Ind Microbiol Biotechnol 19(2):83–86. doi:10.1038/sj.jim.2900434
28. Li CX, Florova G, Akopiants K, Reynolds KA (2004) Crotonyl-coenzyme A reductase provides methylmalonyl-CoA precursors for monensin biosynthesis by *Streptomyces cinnamonensis* in an oil-based extended fermentation. Microbiology 150(Pt 10):3463–3472. doi:10.1099/mic.0.27251-0
29. Martens-Lobenhoffer J, Bode-Boeger SM (2014) Mass spectrometric quantification of L-arginine and its pathway related substances in biofluids: the road to maturity. J Chromatogr, B: Anal Technol Biomed Life Sci 964:89–102. doi:10.1016/j.jchromb.2013.10.030
30. Milrad de Forchetti SR, Cazzulo JJ (1976) Some properties of the pyruvate carboxylase from *Pseudomonas fluorescens*. J Gen Microbiol 93(1):75–81
31. Peters-Wendisch PG, Schiel B, Wendisch VF, Katsoulidis E, Mockel B, Sahm H, Eikmanns BJ (2001) Pyruvate carboxylase is a major bottleneck for glutamate and lysine production by *Corynebacterium glutamicum*. J Mol Microbiol Biotechnol 3(2):295–300
32. Reeves AR, Cernota WH, Brikun IA, Wesley RK, Weber JM (2004) Engineering precursor flow for increased erythromycin production in *Aeromicrobium erythreum*. Metab Eng 6(4):300–312. doi:10.1016/j.ymben.2004.03.003
33. Ruan X, Stassi D, Lax SA, Katz L (1997) A second type-I PKS gene cluster isolated from *Streptomyces hygroscopicus* ATCC 29253, a rapamycin-producing strain. Gene 203(1):1–9. doi:10.1016/s0378-1119(97)00450-2
34. Schmittgen TD, Livak KJ (2008) Analyzing real-time PCR data by the comparative C-T method. Nat Protoc 3(6):1101–1108. doi:10.1038/nprot.2008.73
35. Sehgal SN, Baker H, Vezina C (1975) Rapamycin (AY-22,989), a new antifungal antibiotic. II. Fermentation, isolation and characterization. J Antibiot (Tokyo) 28(10):727–732
36. Sibarani NE, Gorman MA, Dogovski C, Parker MW, Perugini MA (2010) Crystallization of dihydrodipicolinate synthase from a clinical isolate of *Streptococcus pneumoniae*. Acta Crystallogr Sect F: Struct Biol Cryst Commun 66(Pt 1):32–36. doi:10.1107/s174430910904771x
37. Singh BP, Behera BK (2009) Regulation of tacrolimus production by altering primary source of carbons and amino acids. Lett Appl Microbiol 49(2):254–259. doi:10.1111/j.1472-765X.2009.02652.x
38. Sinha R, Singh S, Srivastava P (2014) Studies on process optimization methods for rapamycin production using *Streptomyces hygroscopicus* ATCC 29253. Bioprocess Biosyst Eng 37(5):829–840. doi:10.1007/s00449-013-1051-y
39. Tang L, Zhang YX, Hutchinson CR (1994) Amino acid catabolism and antibiotic synthesis: valine is a source of precursors for macrolide biosynthesis in *Streptomyces ambofaciens* and *Streptomyces fradiae*. J Bacteriol 176(19):6107–6119
40. Tsotsou GE, Barbirato F (2007) Biochemical characterisation of recombinant *Streptomyces pristinaespiralis* L-lysine cyclodeaminase. Biochimie 89(5):591–604. doi:10.1016/j.biochi.2006.12.008
41. Wentzel A, Sletta H, Consortium S, Ellingsen TE, Bruheim P (2012) Intracellular metabolite pool changes in response to nutrient depletion induced metabolic switching in *Streptomyces coelicolor*. Metabolites 2(1):178–194. doi:10.3390/metabo2010178
42. Wood CE, Giroux D, Gridley K (2003) Fetal brain regional responses to cerebral hypoperfusion: modulation by estrogen. Brain Res 993(1–2):84–89. doi:10.1016/j.brainres.2003.09.001
43. Xia J, Wishart DS (2010) MetPA: a web-based metabolomics tool for pathway analysis and visualization. Bioinformatics 26(18):2342–2344. doi:10.1093/bioinformatics/btq418
44. Xia J, Wishart DS (2011) Web-based inference of biological patterns, functions and pathways from metabolomic data using MetaboAnalyst. Nat Protoc 6(6):743–760. doi:10.1038/nprot.2011.319
45. Xia M, Huang D, Li S, Wen J, Jia X, Chen Y (2013) Enhanced FK506 production in *Streptomyces tsukubaensis* by rational feeding strategies based on comparative metabolic profiling analysis. Biotechnol Bioeng 110(10):2717–2730. doi:10.1002/bit.24941
46. Xu ZN, Shen WH, Chen XY, Lin JP, Cen PL (2005) A high-throughput method for screening of rapamycin-producing strains of *Streptomyces hygroscopicus* by cultivation in 96-well microtiter plates. Biotechnol Lett 27(15):1135–1140. doi:10.1007/s10529-005-8463-y
47. Yu S, Huang D, Wen J, Li S, Chen Y, Jia X (2012) Metabolic profiling of a *Rhizopus oryzae* fumaric acid production mutant generated by femtosecond laser irradiation. Bioresour Technol 114:610–615. doi:10.1016/j.biortech.2012.03.087
48. Zhao S, Huang D, Qi H, Wen J, Jia X (2013) Comparative metabolic profiling-based improvement of rapamycin production by *Streptomyces hygroscopicus*. Appl Microbiol Biotechnol 97(12):5329–5341. doi:10.1007/s00253-013-4852-7

49. Zhou LN, Yao WF, Liu J, Shang J, Shan MQ, Zhang L, Ding AW (2013) Protective effect of different solvent extracts from platycladi cacumen carbonisatum on LPS-induced human umbilical vein endothelial cells damage. Zhongguo Zhong Yao Za Zhi 38(22):3933–3938

50. Zhu X, Zhang W, Chen X, Wu H, Duan Y, Xu Z (2010) Generation of high rapamycin producing strain via rational metabolic pathway-based mutagenesis and further titer improvement with fed-batch bioprocess optimization. Biotechnol Bioeng 107(3):506–515. doi:10.1002/bit.22819